Analytical Methods

PAPER

View Article Online
View Journal

Cite this: DOI: 10.1039/c4ay00919c

Sub-micron proximal probe thermal desorption and laser mass spectrometry on painting cross-sections

Shawn C. Owens,[a] Jacob A. Berenbeim,[a] Catherine Schmidt Patterson,[b] Eoghan P. Dillon[c] and M. S. de Vries*[a]

Received 16th April 2014
Accepted 19th August 2014

DOI: 10.1039/c4ay00919c

www.rsc.org/methods

We demonstrate sub-micron, atomic force microscopy (AFM) proximal probe desorption of organic dyes, and subsequent detection *via* laser mass spectrometry. A nanothermal analysis (nano-TA) probe tip in contact with a surface is heated (10 000 °C s^{-1}) to induce thermal desorption, creating depression sizes ranging from 360–1500 nm in diameter and 20–100 nm in depth. Desorbed material is drawn through a heated capillary *via* vacuum, and deposits onto a graphite sample bar. Laser desorption, followed by supersonic jet-cooling and either resonant two-photon ionization (R2PI) or non-resonant ionization mass spectrometry is used to characterize the transferred material. Individual, microscopic layers of organic dyes within painting cross-sections were successfully analyzed using this new approach. Separating the AFM thermal desorption step from the detection step allows for the use of analytical techniques appropriate for individual samples of material, desorbed with high spatial resolution.

Introduction

The analysis of cultural heritage materials presents a number of challenges that limit the range of analytical techniques available for use, these obstacles include: limited and extremely small samples, complexity of sample structure, the importance of maintaining spatial integrity and, most notably, the rarity of the samples. These limitations present unique challenges for the identification of organic dyes, particularly in paintings that may have multiple paint layers due to the artist's technique as well as subsequently applied restoration layers. These materials are often examined by analysis of microscopic painting cross-sections in which complex mixtures and thin (often only a few microns) layers of organic material are commonly encountered. Elucidating the nature of these organic compounds with high spatial resolution may help clarify aspects of a painting's history; and can assist in the painting's conservation since these molecules are often prone to degradation from moisture, light, or other environmental conditions. Therefore, there is a need for analytical techniques that can provide spatially resolved, molecularly-specific, and unambiguous identification of organic compounds in cultural heritage materials.

A number of analytical techniques have been used to identify the materials in painting cross-sections. A variety of spatially resolved spectroscopic and mass spectrometric techniques developed to identify elements and general functional groups are well established and extensively used in cultural heritage science,[1,2] but they are not optimized for detailed analysis of molecular composition. For example, secondary ion mass spectrometry (SIMS) can attain spatial resolutions on the order of 10–50 nm for elemental analysis, and has also been extended to some organic colorants as well.[3,4] Due to the inherent fragmentation of organics with SIMS, many organic pigments that have similar molecular weights or structures can be difficult to distinguish from each other. Scanning electron microscopy/energy dispersive X-ray spectroscopy (SEM-EDS) provides high spatial resolution, but being an elemental analysis technique it is better suited to the identification of inorganic species than organic components.[5] Micro X-ray fluorescence (μ-XRF) is a commonly used, often mobile, instrument capable of ~65–100 μm spatial resolutions,[6,7] but is also limited to elemental analysis. Molecular identification of organic molecules can be accomplished using spectroscopic techniques-such as a recent example combining laser ablation and surface-enhanced Raman spectroscopy (SERS)[8]-but, relatively broad fluorescence signals masking organic bands in complex mixtures of natural organic dyes can often limit identification to broad classes of organic components. In addition, a spatial resolution of ~10 μm limits its use in many paint cross-section applications. Raman microscopy and Raman mapping can also provide spatially resolved (~1–2 μm) molecularly specific

[a]University of California Santa Barbara, Department of Chemistry and Biochemistry, Santa Barbara, CA, USA. E-mail: devries@chem.ucsb.edu; Fax: +1 805 893 4120; Tel: +1-805-893-4720

[b]Getty Conservation Institute, 1200 Getty Center Drive, Suite 700, Los Angeles, CA, USA. E-mail: cpatterson@getty.edu; Fax: +1 310 440 7711; Tel: +1 310 440 6232

[c]Anasys Instruments, 325 Chapala St, Santa Barbara, CA, USA. E-mail: eoghan@anasysinstruments.com; Fax: +1 805 730 3300; Tel: +1 805 730 3310

identification, but still has difficulty to differentiate spectroscopically similar molecules that are common in organic colorants.[9,10] Fourier transform infrared spectroscopy (FTIR) microscopy can provide specific identification of both organic and inorganic compounds, and the continued development of attenuated total reflection (ATR) FTIR (~6 μm),[11] synchrotron-based FTIR (<1 μm),[12,13] and FTIR imaging techniques (~10–15 μm)[14,15] have begun to address the challenges of thin layers and the need for spatial specificity. Still, FTIR either lacks the spatial or spectroscopic resolution for organic containing cross-sections, or requires the use of synchrotron facilities. An additional possibility is a form of laser desorption mass spectrometry (LDMS) that avoids many problems associated with analyzing complex mixtures, and is a valuable tool in the identification of several organic pigments.[16] However, fragmentation caused by LDMS can complicate categorical identification of certain pigments in addition to being limited by a spatial resolution of ~2–4 μm.[17] Ultimately, none of these techniques maintain both high spatial resolution and high selectivity.

Recently, Berkel and coworkers reported nanometer scale atomic force microscopy (AFM) proximal probe thermal desorption (AFM-TD) (Anasys Instruments, Santa Barbara) of organic molecules, and subsequent detection *via* electrospray ionization mass spectrometry (ESI-MS).[18] Additionally, the Zenobi group developed an active plasma source allowing for ambient pressure ionization mass spectrometry on direct analysis of desorbed material.[19] We further extend this combination of AFM proximal probe AFM-TD and MS by decoupling the AFM step from the MS step. In our approach we collect sub-micron size samples through AFM proximal probe AFM-TD, followed by separate analysis with resonant two photon ionization (R2PI) coupled with mass spectrometry. While ESI-MS is well suited for mass spectrometry of unknown compounds, R2PI can identify and selectively ionize specific molecules. So, when particular compounds can be targeted, R2PI is well suited for the complicated samples typically present in cultural heritage artifacts. We note that the inherent optical resolution in low temperature laser spectroscopy such as R2PI can often be much higher than the mass resolution in a typical mass spectrometer (MS).[20] We also employ non-resonant LDMS to demonstrate the flexibility created by decoupling AFM-TD and MS. Our approach consists of a two-step process: (1) sample collection, in which an AFM-mounted microscope is used to identify features, proximal probe AFM-TD is performed at selected locations and desorbed material is transferred to a sample bar through a capillary, and (2) sample analysis, in which the bar with desorbed material is transferred to the laser mass spectrometer for laser desorption of molecules, followed by jet cooling of the desorbed molecules, R2PI and finally detection in a time-of-flight MS. While normally the spatial resolution of laser desorption is limited by the laser spot size of approximately 1 μm,[17] the combination with the preceding AFM-TD sampling step makes it possible to reach a spatial resolution of ~0.5 μm.

Experimental

Solvents and chemicals

The dye alizarin crimson dark (Kremer Pigment 2361), and the synthetic organic pigments PV19 (Pigment Violet 19, Ciba) and PO43 (Pigment Orange 43, Clariant) were obtained from the Getty Conservation Institute's Reference Collection. Alizarin 97% pure was obtained from ACROS Organics. Binding media used for paint samples were egg yolk for alizarin crimson, and multi-purpose white glue (Elmer's Glue) for the synthetic organic pigments. Egg yolks were taken from whole chicken eggs obtained indiscriminately from the grocery store. Technovit 2000 LC light curing resin (Heraeus Kulzer GmbH & Co. KG) was used for the preparation of painting cross-section samples. Caffeine (anhydrous) was obtained from Sigma Aldrich to prepare a sample to test the analytical method prior to cross-section analysis. HPLC grade methanol was obtained from Fischer Chemical.

Sample preparation

Two methods are employed to make samples; thin film deposition on a silica wafer and resin embedding of painting cross-sections. Using a home-built spin coater, a 0.3–0.5 mL aliquot of 0.02 M caffeine in methanol is deposited onto a silica substrate by a syringe and spun off at 5000 rpm for 1 s. To prepare samples from which a cross-section could be made, individual layers of paint (arbitrary thickness) are applied to a modern gesso-prepared board (Ampersand gesso board, acrylic gesso surface) and allowed to dry. Incisions are made using a scalpel in the dried paint to reveal and remove a piece of the painted surface in cross-section, before embedding in resin and curing under blue light. These samples are dry-polished iteratively by hand (Micro-Mesh, Micro Surface Finishing Products, Inc).

Instrumentation

The atomic force microscopy-thermal desorption (AFM-TD) experiments are carried out using an Anasys Instruments afm+®. The system allows for high spatial resolution nanothermal analysis (nanoTA), achieved by the use of Thermalever™ AFM probes. These probes are batch-fabricated silicon AFM probes with a resistive heater element integrated into the end of the cantilever, allowing for the controlled heating of the probe. Initial nanoTA ramps were performed within each homogeneous sampling area to determine a voltage ramp profile, and to indicate the thermal transitions of the material being sampled. A maximum probe temperature defines the voltage ramp profile and is set to a corresponding bulk phase transition. The probe is ramped to the nanoTA maximum temperature at a rate of 10 000 °C s^{-1} and a typical maximum desorption temperature of 400 °C can be reached in tens of μs. The probe is calibrated by increasing the voltage to the probe while on the surface of three polymeric materials with known melting temperatures: PCL, PE and PET. At each material's melting point, the probe penetrates into the sample surface and the voltage value can then be converted to °C, as the melt temperatures of these polymers have been well characterized.

For the samples analyzed, spot sampling time is determined by a ramp rate of 100 V s^{-1}, but is typically in the range of 25–50 ms. Material is repeatedly desorbed from the sample surface at a sequence of different spots within each sample or layer within a sample (Table 1).

As shown in Fig. 1, the resulting desorption plume is drawn *via* vacuum through a stainless steel (SS) capillary, and into an isolated sample collection box, where it deposits onto a graphite sample bar. For caffeine sampling a SS 6″ × 0.05″ OD × 0.03″ ID capillary is pumped at a flow rate of ~150 mL s^{-1}. For pigments, a SS 6″ × 0.05″ OD × 0.033″ ID capillary is pumped at a flow rate of ~215 mL s^{-1}. The larger diameter capillary served to increase the flow rate. The capillary is heated to 90 °C to reduce condensation of the desorbed material during the transfer. The capillary is positioned approximately 200–500 μm from the AFM tip in order to maximize the amount of desorbed material drawn through the capillary and onto the graphite sample bar; limiting this distance avoids interference from mechanical vibrations caused by the continuous pumping of the sample collection box. Since the analysis step is separated from the analysis step, it is possible to optimize the sampling geometry and conditions for maximum collection. In real time direct inlet mass spectrometry, for example, this is harder to achieve because the flow rate affects the ionization efficiency. Numerous desorption spots from the same local area (*e.g.* paint layer) are deposited additively onto the graphite bar in order to maximize sample material transfer ensuring enough material for subsequent mass spectral analysis. The graphite bar can be translated allowing deposition of different spots across the bar. The entire sample collection box is on a 3-axis stage to give full movement for positioning the capillary nearest the AFM tip.

The experimental setup for mass spectrometry has been described elsewhere.[20] The sample bar is loaded into a high vacuum chamber, where it is positioned directly in front of a pulsed nozzle. The sample bar can be translated for successive laser shots on different locations. Material is laser desorbed from the sample bar by light from a Continuum MiniLite 1064 nm Nd:YAG laser, which is attenuated to minimize fragmentation and focused to a slit approximately 1 × 5 mm, within 5 mm of the nozzle. The desorbed material is entrained in a pulsed supersonic argon stream controlled by an ACPV2 pulsed cantilever piezovalve[21] with an opening diameter of 300 μm and an concave conical shape with a full angle of 40°, at a backing pressure of 6 bar. The Ar molecular beam is skimmed before entering a source region where it is intersected by laser beam(s) and photo-ionized.

Two ionization techniques are employed: resonance enhanced two photon ionization (R2PI) and non-resonant ionization. R2PI uses a first photon from a Lumonics tunable dye laser to resonantly excite a molecule to an electronic excited state, followed immediately by a second photon from either the same or a different dye laser which ionizes the molecule. We have previously reported the spectroscopy of caffeine,[11] which allows tuning the dye laser to a specific resonance in order to selectively ionize it and record the mass spectrum. The R2PI of caffeine was carried out with a set wavelength of 281.635 nm (1.1 mJ per pulse). Non-resonant ionization was carried out for all pigments using a 193 nm excimer laser (~4 mJ per pulse). All ions are characterized in a reflectron time-of-flight mass spectrometer. Typical mass resolution ($m/\Delta m$) is 700 or higher. The duty cycle of the experiment is 10 Hz.

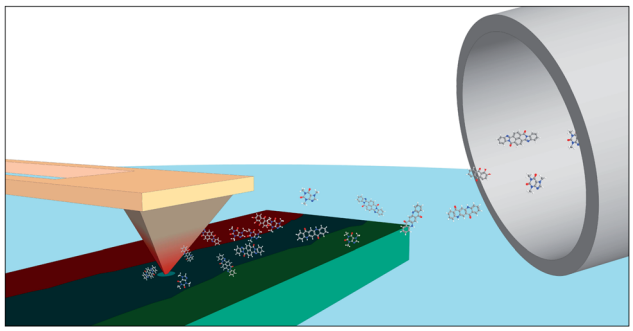

Fig. 1 Representation of AFM-TD process and resulting plume being drawn into the capillary.

Results and discussion

A topographic image was taken before and after each experiment to investigate the AFM-TD depression sizes as well as any other changes to the morphology of the sample. Table 1 lists the complete set of molecules that were successfully transferred and identified, along with the number of times the tip was heated to induce desorption (AFM-TD Events) for each sample, as well as desorption depression characteristics. Successful AFM-TD appeared to be dependent on the thermal characteristics of the binding medium, as opposed to the pigment within that binding medium.

To determine the viability of separate AFM-TD and mass spectrometric steps, caffeine served for initial experiments as we have previously reported laser desorption jet-cooling R2PI-MS of caffeine, and the R2PI spectroscopy of this molecule is well known.[22] Generally R2PI mass spectral analysis is only possible with prior knowledge of the R2PI spectrum for the jet-cooled molecule. Since the spectroscopic peaks are dependent

Table 1 AFM-TD Sample Characteristics

Molecule	Molecular weight (g mol^{-1})	TD events	Crater diameter (nm)	Crater depth (nm)	Crater volume (nm^3)
Caffeine	194.19	55–85	360	20–200	6.8×10^5–6.8×10^6
Alizarin	240.21	15	750	700	1.0×10^8
PV19	312.32	10	750–1500	800–1000	1.2×10^8–5.9×10^8
PO43	412.41	10	800–1000	200–400	3.4×10^7–1.0×10^8

on, and extremely sensitive to, structure this technique allows for indisputable identification of molecules by simultaneous spectroscopic and fragment-free mass spectrometric characterization. Fig. 2a shows the R2PI spectrum of caffeine obtained by scanning the tunable excitation laser.[22] The photo-ionization step adds significantly to the molecular selectivity of the analysis, the strong absorption at 281.635 nm was used for R2PI-MS experiments.

A number of AFM-TD events from a caffeine-coated silica wafer were transferred to a graphite sample bar as 3 separate spots (AFM-TD events on each spot: (1) 55 (2) 75 (3) 85). Fig. 2b illustrates the R2PI-MS corresponding to material from spot 1 on the sample bar. The parent peak of caffeine is seen at *m*/*z* 194, indicating a successful transfer of the sample following AFM-TD (Ar, the carrier gas, can be seen at *m*/*z* 40). Note the absence of unrelated peaks observed from either AFM-TD fragmentation or the laser desorption of the graphite matrix, illustrating the highly selective nature of R2PI-MS. To verify caffeine was present in each spot on the sample bar, the signal of caffeine (*i.e.* the intensity at *m*/*z* 194.19) was monitored as the sample bar was translated, in order to laser desorb from each of the 3 spots. Fig. 3 shows a back and forth scan. After spot 3 was analyzed, the direction of the bar was reversed in order to laser desorb again from same spots 2 and 1. The signal spike seen in spot 3 is due to an increase in the bar speed reversing directions, exposing fresh sample at a faster rate and resulting in a slight signal increase. The rate was returned to a slower speed after the increased signal seen in spot 3.

The fact that signal from spots 2 and 1 can be detected on the second pass demonstrates that complementary analytical techniques can be performed on the same sample spot more than once.

Following successful application to the well-characterized caffeine system, the AFM-TD technique was next applied to more challenging samples – a traditional organic colorant and modern synthetic pigments prepared as mounted cross-sections – in order to determine whether the overall approach is reasonable for samples of these types.

Fig. 4a shows a microscope image of a cross-section containing the traditional red organic colorant alizarin crimson.

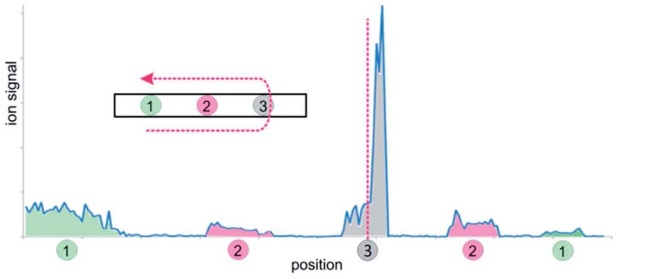

Fig. 3 Caffeine parent peak intensity monitored while translating sample bar back and forth over three spots in order 1-2-3-2-1. Colored peaks correspond to deposited spots on sample bar from AFM-TD. The red dashed-line represents the point at which the direction of the sample bar translation was reversed.

Following AFM-TD of the alizarin layer, we performed laser desorption mass spectrometry using a 193 nm excimer laser for ionization. The parent peak corresponding to the alizarin chromophore can be seen at *m*/*z* 240.21. Several other species also appear, indicative of the complex nature of these natural organic dyes. Analogous non-resonant laser ionization experiments with standard alizarin crimson dye (without the AFM-TD step) were performed to determine whether additional fragments were created in the AFM-TD heating step. The results indicated that though some additional fragmentation did occur, the vast majority of the mass peaks were identical. The limited additional fragmentation was likely due to thermal fragmentation during the relatively slow heating rate of the AFM-TD process. Nonetheless, in each case, intact molecules were successfully thermally desorbed, transferred, and detected in a mass spectrometer. As evident by the small size of the sampling depressions (750 nm diameter), several samples within even the thinnest paint layers could be obtained while maintaining the bulk of the cross-sections for further analytical work.

To complement work done on the natural organic dye, we performed additional experiments using modern synthetic pigments PV19 and PO43. Fig. 5a shows a microscope image of a cross-section consisting of a sequence of layers (from bottom to top: titanium white, PV19, PO43, PY151, PR254).

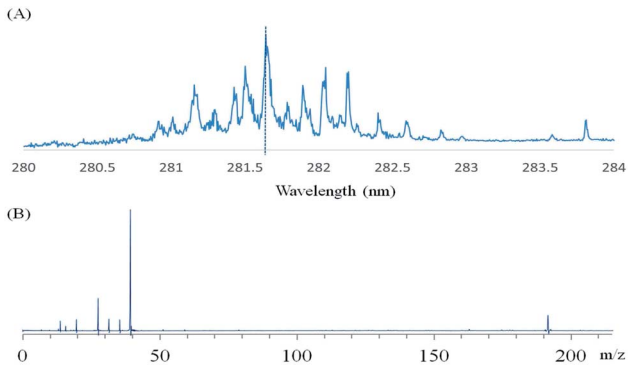

Fig. 2 (A) R2PI spectrum of caffeine, dashed line corresponds to 281.635 nm (B) R2PI mass spectrum of caffeine, parent peak located at *m*/*z* 194.19.

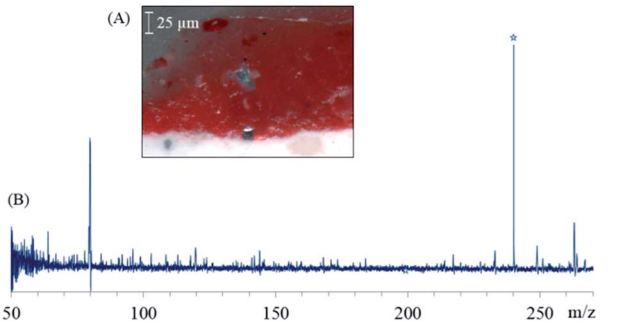

Fig. 4 (A) Microscope image of alizarin crimson dye layer, with white substrate below (B) non-resonant ionization mass spectrum from alizarin dye layer. Star denotes parent mass peak.

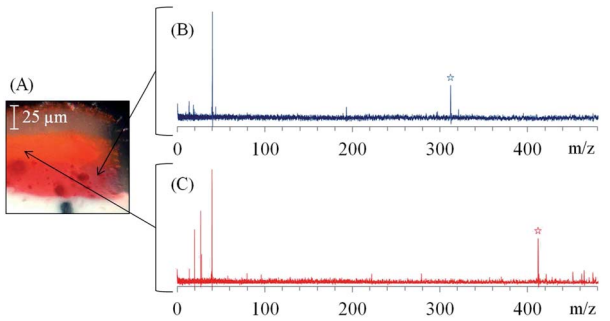

Fig. 5 (A) Microscope image of synthetic dye cross section. The sequence of layers from bottom to top: PV19, PO43, PY151 and PR254. (B) Mass spectrum (non-resonant) obtained from PV19 dye layer and (C) non-resonant ionization mass spectrum (non-resonant) from PO43 dye layer. Stars denotes parent mass peaks.

Fig. 5b shows the mass spectrum produced from the layer of PV19, where the parent peak is visible at *m*/*z* 312.32. Fig. 5c shows the mass spectrum of the PO43 layer. The parent peak of PO43 can be seen at *m*/*z* 412.41. There was little indication of any fragmentation in the modern synthetic pigments, although it is worth noting these were pure standards. In contrast, traditional colorants such as alizarin crimson are complex mixtures of molecules because they are often obtained through plant and animal matter, and consequently have complex spectra. Desorption depression sizes in the modern synthetics ranged from 750–2500 μm, likely due to melting of the paint medium (Elmer's Glue) by the radiant heat from the probe tip. There was no indication of any PV19 desorption or detection in the PO43 layer, nor *vice versa*, demonstrating the absence of cross contamination and confirming the high spatial resolution.

Conclusions

We have demonstrated a new approach for coupling proximal probe AFM-TD and subsequent chemical analysis in separate steps. This approach allows the use of a diverse set of techniques adapted to the characteristics of each individual sample on a case by case basis. By using R2PI mass spectrometry for the separate analysis step, this new sample collection method provides a format for unambiguously identifying specific organic colorants. This approach should be particularly well-suited for samples in which the spatial resolution of other available analytical techniques is insufficient to probe, such as thin layers or small inclusions of an unknown organic material. Further work is needed to catalogue the response of different target compounds of interest in the sampling step as well as their spectra for R2PI analysis. Forthcoming work will be extended to identify different binding media, including oil, gum, varnishes and more complex mixtures of organic and inorganic pigments, as these are more representative of authentic cultural heritage artifacts. This method can also be extended to other fields of research which face similar challenges in spatially resolved organic analysis.

Acknowledgements

The authors thank Dr Karen Trentelman and Alan Phenix for their exceptional contributions to this work. We are also grateful to Kevin Kjoller, Roshan Shetty and Anasys Instruments for the generous donation of their time and research facilities. This material is based upon work supported by the National Science Foundation under CHE 1301305 and CHE 1018804.

Notes and references

1 G. Spoto, A. Torrisi and A. Contino, *Chem. Soc. Rev.*, 2000, **29**, 429–439.
2 G. Spoto and G. Grasso, *TrAC, Trends Anal. Chem.*, 2011, **30**, 856–863.
3 A. Adriaens and M. G. Dowsett, *Appl. Surf. Sci.*, 2006, **252**, 7096–7101.
4 C. S. Deroo and R. A. Armitage, *Anal. Chem.*, 2011, **83**, 6924–6928.
5 C. Genestar and C. Pons, *Anal. Bioanal. Chem.*, 2005, **382**, 269–274.
6 G. Vittiglio, S. Bichlmeier, P. Klinger, J. Heckel, W. Fuzhong, L. Vincze, K. Janssens, P. Engström, A. Rindby, K. Dietrich, D. Jembrih-Simbürger, M. Schreiner, D. Denis, A. Lakdar and A. Lamotte, *Nucl. Instrum. Methods Phys. Res., Sect. B*, 2004, **213**, 693–698.
7 K. Trentelman, M. Bouchard, M. Ganio, C. Namowicz, C. Schmidt and M. Walton, *X-Ray Spectrom.*, 2010, 159–166.
8 P. S. Londero, J. R. Lombardi and M. Leona, *Anal. Chem.*, 2013, **85**, 5463–5467.
9 G. Paternoster, R. Rinzivillo, F. Nunziata, E. M. Castellucci, C. Lofrumento, A. Zoppi, A. C. Felici, G. Fronterotta, C. Nicolais, M. Piacentini, S. Sciuti and M. Vendittelli, *J. Cult. Herit.*, 2005, **6**, 21–28.
10 P. Vandenabeele, B. Wehling, L. Moens, H. Edwards, M. De Reu and G. Van Hooydonk, *Anal. Chim. Acta*, 2000, **407**, 261–274.
11 S. Prati, E. Joseph, G. Sciutto and R. Mazzeo, *Acc. Chem. Res.*, 2010, **43**, 792–801.
12 G. D. Smith, *J. Am. Inst. Conserv.*, 2003, **42**, 399–406.
13 J. Mass, J. Sedlmair, C. S. Patterson, D. Carson, B. Buckley and C. Hirschmugl, *Analyst*, 2013, **138**, 6032–6043.
14 E. Joseph, S. Prati, G. Sciutto, M. Ioele, P. Santopadre and R. Mazzeo, *Anal. Bioanal. Chem.*, 2010, **396**, 899–910.
15 E. Joseph, C. Ricci, S. G. Kazarian, R. Mazzeo, S. Prati and M. Ioele, *Vib. Spectrosc.*, 2010, **53**, 274–278.
16 D. P. Kirby, N. Khandekar, K. Sutherland and B. A. Price, *Int. J. Mass Spectrom.*, 2009, **284**, 115–122.
17 L. I. Grace, A. Abo-Riziq and M. S. deVries, *J. Am. Soc. Mass Spectrom.*, 2005, **16**, 437–440.
18 O. S. Ovchinnikova, M. P. Nikiforov, J. A. Bradshaw, S. Jesse and G. J. Van Berkel, *ACS Nano*, 2011, **5**, 5526–5531.
19 M. M. Nudnova, L. Zhu and R. Zenobi, *Rapid Commun. Mass Spectrom.*, 2012, **26**, 1447–1452.

20 G. Meijer, M. S. Devries, H. E. Hunziker and H. R. Wendt, *Appl. Phys. B: Photophys. Laser Chem.*, 1990, **51**, 395–403.
21 D. Irimia, D. Dobrikov, R. Kortekaas, H. Voet, D. A. van den Ende, W. A. Groen and M. H. M. Janssen, *Rev. Sci. Instrum.*, 2009, 80.
22 M. P. Callahan, Z. Gengeliczki, N. Svadlenak, H. Valdes, P. Hobza and M. S. de Vries, *Phys. Chem. Chem. Phys.*, 2008, **10**, 2819–2826.

